Distinct Gene Expression Profiles of Viral- and Nonviral-Associated Merkel Cell Carcinoma Revealed by Transcriptome Analysis

Paul W. Harms[1,2], Rajiv M. Patel[1,2], Monique E. Verhaegen[2], Thomas J. Giordano[1], Kevin T. Nash[2], Craig N. Johnson[3], Stephanie Daignault[4], Dafydd G. Thomas[1], Johann E. Gudjonsson[2], James T. Elder[2,5], Andrzej A. Dlugosz[2,6], Timothy M. Johnson[2], Douglas R. Fullen[1,2] and Christopher K. Bichakjian[2]

Merkel cell carcinoma (MCC) is an aggressive cutaneous neuroendocrine tumor with high mortality rates. Merkel cell polyomavirus (MCPyV), identified in the majority of MCCs, may drive tumorigenesis via viral T antigens. However, the mechanisms underlying pathogenesis in MCPyV-negative MCCs remain poorly understood. To nominate genes contributing to the pathogenesis of MCPyV-negative MCCs, we performed DNA microarray analysis on 30 MCCs. The MCPyV status of MCCs was determined by PCR for viral DNA and RNA. A total of 1,593 probe sets were differentially expressed between MCPyV-negative and MCPyV-positive MCCs, with significant differential expression defined as at least a 2-fold change in either direction and a *P*-value $\leqslant 0.05$. MCPyV-negative tumors showed decreased *RB1* expression, whereas MCPyV-positive tumors were enriched for immune response genes. Validation studies included immunohistochemistry demonstration of decreased RB protein expression in MCPyV-negative tumors and increased peritumoral CD8+ T lymphocytes surrounding MCPyV-positive tumors. In conclusion, our data suggest that loss of *RB1* expression may have an important role in the tumorigenesis of MCPyV-negative MCCs. Functional and clinical validation studies are needed to determine whether this tumor-suppressor pathway represents an avenue for targeted therapy.

Journal of Investigative Dermatology (2013) **133,** 936–945; doi:10.1038/jid.2012.445; published online 6 December 2012

INTRODUCTION

Merkel cell carcinoma (MCC) is an aggressive neuroendocrine tumor of the skin with high rates of recurrence, metastasis, and mortality. The incidence of MCC has nearly tripled in the past 20 years, and this malignancy is more prevalent in the immunosuppressed and the elderly. The 5-year overall survival from the time of diagnosis is 30–64%. Survival decreases upon metastasis to lymph nodes, distant skin sites, or distant organs (Bichakjian *et al.*, 2007).

There is an increased risk for MCC in solid organ transplant recipients, chronic lymphocytic leukemia patients, and HIV-infected patients, suggesting an infectious etiology for this malignancy (Kuhajda *et al.*, 1986; Penn and First, 1999; Engels *et al.*, 2002; Bhatia *et al.*, 2011). The DNA of Merkel cell polyomavirus (MCPyV), has been identified in ~80% of MCCs (Feng *et al.*, 2008; Foulongne *et al.*, 2008; Kassem *et al.*, 2008; Becker *et al.*, 2009; Garneski *et al.*, 2009; Katano *et al.*, 2009; Bhatia *et al.*, 2011; Brewer *et al.*, 2012). MCPyV may contribute to tumorigenesis via a truncated large T antigen (LTAg) and small T antigen (STAg), which inhibit the tumor-suppressor RB and promote signaling by the mammalian target of rapamycin pathway, respectively (Shuda *et al.*, 2008, 2011; Houben *et al.*, 2012). The mechanisms of tumorigenesis specific to MCPyV-negative tumors are less well understood, although altered expression of RB, p53, and/or c-KIT suggest that these molecules may have a role (Bhatia *et al.*, 2010b; Sihto *et al.*, 2011; Waltari *et al.*, 2011).

To our knowledge, transcriptional profiles of MCPyV-negative and MCPyV-positive tumors have not been compared. To nominate candidate genes involved in MCPyV-independent MCC tumorigenesis, we performed DNA microarray analysis of MCC tumors and correlated profiling results with MCPyV tumor status.

[1]*Department of Pathology, University of Michigan Medical Center, Ann Arbor, Michigan, USA;* [2]*Department of Dermatology, University of Michigan Medical Center, Ann Arbor, Michigan, USA;* [3]*Sequencing Core, University of Michigan Medical Center, Ann Arbor, Michigan, USA;* [4]*Biostatistics Core, Comprehensive Cancer Center, University of Michigan, Ann Arbor, Michigan, USA;* [5]*Ann Arbor Veterans Affairs Hospital, Ann Arbor, Michigan, USA and* [6]*Department of Cell and Developmental Biology, University of Michigan Medical Center, Ann Arbor, Michigan, USA*

Correspondence: Paul W. Harms, Department of Pathology, University of Michigan, M3260, Medical Science I, 1301 Catherine Street, Ann Arbor, Michigan 48109-0602, USA. E-mail: paulharm@med.umich.edu

Abbreviations: BCC, basal cell carcinoma; GO, Gene Ontology; KEGG, Kyoto Encyclopedia of Genes and Genomes; LTAg, large T antigen; MCC, Merkel cell carcinoma; MCPyV, Merkel cell polyomavirus; SCC, squamous cell carcinoma; STAg, small T antigen; TIL, tumor-infiltrating lymphocyte

Received 13 July 2012; revised 10 September 2012; accepted 26 September 2012; published online 6 December 2012

RESULTS

Patient demographics

Patient demographic information is summarized in Table 1. The study included 30 tumors from 27 patients (14 men and 13 women) diagnosed with MCC between 2005 and 2010. The mean patient age at diagnosis was 75 years. Two patients were immunosuppressed at the time of diagnosis because of organ transplant. Two additional patients had chronic lymphocytic leukemia.

Transcriptional profiling demonstrates distinct gene expression patterns in MCC compared with other primary cutaneous carcinomas

To characterize gene expression patterns in MCC, we analyzed transcriptional profiles of 19 primary MCCs, 11 metastatic MCCs, 3 MCC cell lines, 4 primary cutaneous squamous cell carcinomas (SCCs), and two basal cell carcinomas (BCCs). Oligonucleotide arrays with over 54,000 probe sets representing over 47,400 transcripts were used. To generate an unsupervised two-dimensional representation of relative gene expression across all tumors, we performed principal component analysis of all probe sets. The resulting principal component analysis plot demonstrated clear distinction of MCCs from SCCs and BCCs, with only one outlier (Figure 1). Cultured MCC cells, which represent a pure population of tumor cells, assorted with MCC tumor specimens. The single MCC outlier case was morphologically similar to other MCC tumors in the cohort, but had lower tumor volume than other samples.

For all analyses, significant differential expression was defined as at least a 2-fold differential expression in either direction, with an adjusted *P*-value of $\leqslant 0.05$. Relative to SCCs, MCCs demonstrated significant differential expression of over 4,000 probe sets (Supplementary Figure S1 and Supplementary Table S1 online, and data not shown), with a false discovery rate of 1.8%. In validation of our approach, our screen identified established diagnostic markers of MCCs including cytokeratin 20, chromogranin A, synaptophysin, and neural cell adhesion molecule 1, as well as known markers for SCCs such as cytokeratin 5/6 and tumor protein 63 (Supplementary Table S1 online). In addition, we observed upregulation of the proposed mechanoreceptor genes Piezo2 (*FAM38B*) and *TRPC1* (Chalfie, 2009; Coste *et al.*, 2010; Garrison *et al.*, 2011). To screen for upregulated genes with potential roles in tumorigenesis, we searched the data set for the term ''oncogene'' in the gene description, and filtered these candidates by literature search to identify genes with known roles in cancer biology. Using this method, we identified potentially protumorigenic genes including *FYN*, *AKT3*, *MYB*, *RAB3B*, *JUND*, and *FEV* (Supplementary Table S1 online) (Peter *et al.*, 1997; Ramsay and Gonda, 2008; Saito *et al.*, 2010; Hers *et al.*, 2011; Nakayama *et al.*, 2012; Tan *et al.*, 2012). In further validation of our data set, we also found upregulation of genes previously reported to be expressed in MCC, including *SOX2*, *BCL2*, *MYCL1*, *VEGFA*, *GPC3*, *ATOH1*, *HIP1*, and *KIT* (Supplementary Table S1 online) (Kennedy *et al.*, 1996; Moll *et al.*, 1996; Plettenberg *et al.*, 1996; Ben-Arie *et al.*, 2000; Leonard *et al.*, 2002; Su *et al.*, 2002; Fernandez-Figueras *et al.*, 2007; Brunner *et al.*, 2008; He *et al.*, 2009; Paulson *et al.*, 2009; Laga *et al.*, 2010; Ames *et al.*, 2011). We also identified upregulation of numerous genes previously described as expressed in benign Merkel cells, including neuronal transcription factors, presynaptic molecules, and ion channels (Supplementary Table S1 online) (Haeberle *et al.*, 2004).

The group of overexpressed or underexpressed genes in MCCs relative to SCCs was assessed for functional clusters by Gene Ontology (GO) analysis, which revealed that MCCs were enriched for gene sets associated with neural differentiation (Supplementary Table S2 online). Comparison with a database of gene expression profiles via parametric gene set analysis revealed similarity between MCCs and tumors including neuroblastoma (Supplementary Figure S2 online).

A comparison of MCCs with BCCs yielded 650 significantly different probe sets. Genes upregulated in BCCs relative to MCCs included the Hedgehog pathway transcripts *GLI1*, *GLI2*, *PTCH1*, and *PTCH2*, as well as the Hedgehog target basonuclin (Supplementary Table S3 online), consistent with the known role of Hedgehog signaling in BCCs (Cui *et al.*, 2004; Kasper *et al.*, 2012).

In silico comparison of MCCs with normal skin demonstrated a significant difference in expression in $>8{,}000$ probe sets, with significant differential expression defined as at least 2-fold differential expression in either direction, with an adjusted *P*-value of $\leqslant 0.05$. The principal component analysis demonstrated clear separation between groups (Supplementary Figure S3 online). We observed differential expression of MCC diagnostic markers, proposed mechanoreceptor genes, and protumorigenic genes (Supplementary Table S4 online).

MCPyV status and clinical features

By PCR detection of MCPyV DNA and RNA, we found that 12/26 (46%) tumors in our cohort were MCPyV-positive and 14/26 (54%) were MCPyV-negative (Supplementary Figure S4 online). There was no significant difference in age at diagnosis and stage at presentation between MCPyV-negative and MCPyV-positive groups. Tumors showed significantly different anatomic distribution by MCPyV status ($P=0.029$). Specifically, 8 of 11 (73%) MCPyV-negative primary tumors were located in the head and neck region and 3 (27%) were on the upper extremities, whereas none was on the lower extremity. In contrast, 3 of 12 (25%) MCPyV-positive primary tumors were located on the head and neck, 4 (33%) on the upper extremity, and 5 (42%) on the lower extremity.

Transcriptional profiling identifies distinct gene expression patterns in MCPyV-negative MCCs

We analyzed gene expression patterns in MCPyV-positive versus MCPyV-negative tumors. By principal component analysis of all probe sets, the majority of MCPyV-positive tumors formed a cluster, which displayed partial overlap with MCPyV-negative tumors (Figure 2). A total of 1,593 probe sets displayed significant differential expression between MCPyV-positive and -negative tumors, with a false discovery rate of 1.9% (Figure 3 and data not shown). By GO and Kyoto Encyclopedia of Genes and Genomes (KEGG) pathway analyses, MCPyV-negative tumors displayed relative

Table 1. Patient and tumor characteristics of profiled cases

								Primary tumor			
Patient no.	Case no.	Tumor type/ source	Gender	Stage at diagnosis	Age at diagnosis	Immuno-suppression	Outcome	Time to outcome (months)	Breslow (mm)	Body site	MCPyV[1]
1	1	Primary/skin	M	3	65	No	DOD	13	⩾7	Shoulder	Negative
2	2	Primary/skin	F	1	82	No	DOC	36	ND	Leg	Positive
3	3	Primary/skin	M	2	88	No	DOC	23	>6	Leg	Positive
4	4	Primary/skin	M	1	81	No	AWED	41	3.3	Forehead	Negative
5	5	Primary/skin	M	1	59	Yes	DOD	15	>2.2	Ear	Negative
6	6	Primary/skin	M	1	70	No	AWED	33	>4	Ear	Negative
7	7	Primary/skin	F	1	85	No	LTFU		5.5	Cheek	Positive
8	8	Primary/skin	F	2	68	No	AWED	37	1.85	Leg	ND
9	9	Primary/skin	F	2	77	No	AWED	7	⩾9	Eyelid	Positive
10	10	Primary/skin	M	3	80	No	AWED	18	⩾4.1	Arm	Positive
11	11	Primary/skin	M	1	59	No	AWED	13	3.8	Arm	Positive
12	12	Primary/skin	F	1	75	No	AWED	12	4.8	Leg	Positive
13	13	Primary/skin	M	1	85	No	AWED	6	9	Hand	Negative
14	14	Primary/skin	F	2	77	No	AWED	12	⩾9	Cheek	Negative
15	15	Primary/skin	M	2	78	No	DOD	7	3.1	Cheek	Negative
16	16	Primary/skin	M	1	80	No	AWED	6	⩾2.5	Leg	Positive
17	17	Metastasis/skin	F	3	78	No	DOD	14	6	Leg	ND
18	18	Metastasis/skin	M	3	85	No	DOD	12	⩾5	Nose	Negative
19	19	Metastasis/skin	M	3	69	No	DOD	17	>6	Temple	Negative
20	20	Metastasis/skin	F	3	67	Yes[2]	DOD	16	10	Forearm	Positive
21	21	Metastasis/skin	F	3	57	No	AWED	62	ND	Foot	Positive
22	22	Metastasis/ parotid	F	3	85	No	DOD	9	18	Cheek	Positive
23	23	Metastasis/ parotid	F	3	90	No	AWED	12	9	Temple	Negative
24	24	Metastasis/LN	F	3	79	No	AWED	20	12	Arm	Positive
25	25	Primary/skin	F	2	85	No	DOD	27	ND	Arm	ND
(25)	26	Metastasis/skin									Negative
26	27	Primary/skin	M	2	53	Yes	AWRD	10	19	Arm	Negative
(26)	28	Metastasis/LN									Negative
27	29	Primary/skin	M	1	71	Yes[2]	DOD	25	4	Neck	Equivocal
(27)	30	Metastasis/ parotid									Negative

Abbreviations: AWED, alive without evidence of disease; AWRD, alive with residual disease; DOC, died of other causes; DOD, died of disease; F, female; LN, lymph node; LTFU, lost to follow-up; M, male; MCPyV, Merkel cell polyomavirus; ND, not determined (because of lack of PCR-quality DNA in the case of MCPyV status).

[1]MCPyV status was determined by PCR of tumor genomic DNA and complementary DNA (cDNA), as described in the text.

[2]Patient with history of chronic lymphocytic leukemia.

upregulation of gene groups associated with Notch signaling and receptor tyrosine kinase signaling, among others (Table 2 and data not shown).

MCPyV-positive tumors are enriched for peritumoral lymphoctyes

The GO and KEGG analyses identified enrichment for a number of gene groups associated with immune response in the MCPyV-positive tumor cohort including *CD3G*, *CD3D*, *ZAP70*, and *IGHM*, suggesting increased presence of tumoral lymphocytes. Thus, we performed immunohistochemical studies to define the immune infiltrate associated with MCPyV-positive tumors. Relative to MCPyV-negative tumors, MCPyV-positive tumors were associated with significantly increased CD8+ cells (fold 14.0, $P=0.01$; Figure 4). There was also a trend toward increased CD3+ cells (fold 3.1,

$P = 0.10$). CD4+ T cells were scant in both MCPyV-positive and MCPyV-negative tumors. CD20+ B cells were variable, with no significant difference between groups (data not shown).

In our cohort, most lymphocytes were in the peritumoral stroma or associated with tumoral vessels, with only a small number of tumor-infiltrating lymphocytes (TILs). We observed a trend toward slightly increased CD8+ TILs in

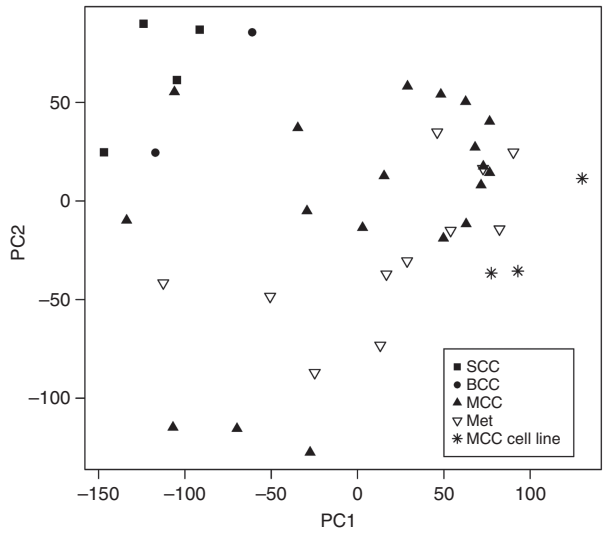

Figure 1. Principal component analysis of Merkel cell carcinoma (MCC) transcriptional profiles relative to MCC cell lines and nonmelanoma skin cancers. MCCs have a distinct expression profile compared with squamous cell carcinomas (SCCs) and basal cell carcinomas (BCCs). Solid squares indicate primary cutaneous SCCs. Solid circles indicate BCCs. Solid triangles indicate MCC primary tumors. Open triangles indicate metastatic MCC tumors (Met). Asterisks indicate MCC cell lines. PC1, principal component 1; PC2, principal component 2.

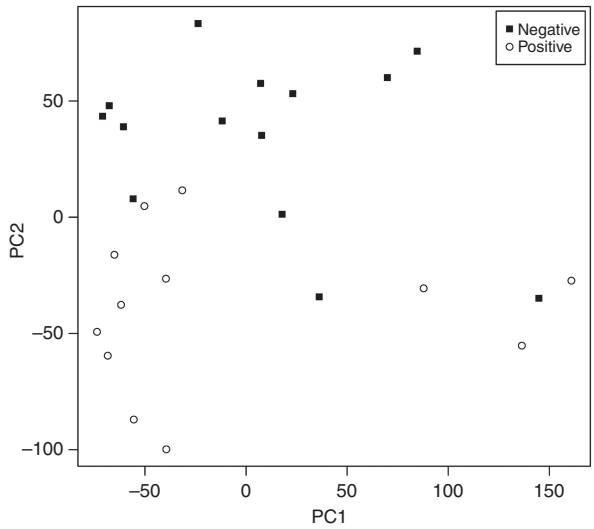

Figure 2. Principal component analysis of Merkel cell carcinoma (MCC) tumors by Merkel cell polyomavirus (MCPyV) status. The majority of MCPyV-positive tumors (open circles) display a distinct cluster that partially overlaps with MCPyV-negative tumors (solid squares). MCPyV-negative tumors are more heterogeneous. Negative: MCPyV T antigen (TAg) DNA and RNA negative. Positive: TAg DNA and RNA positive. PC1, principal component 1; PC2, principal component 2.

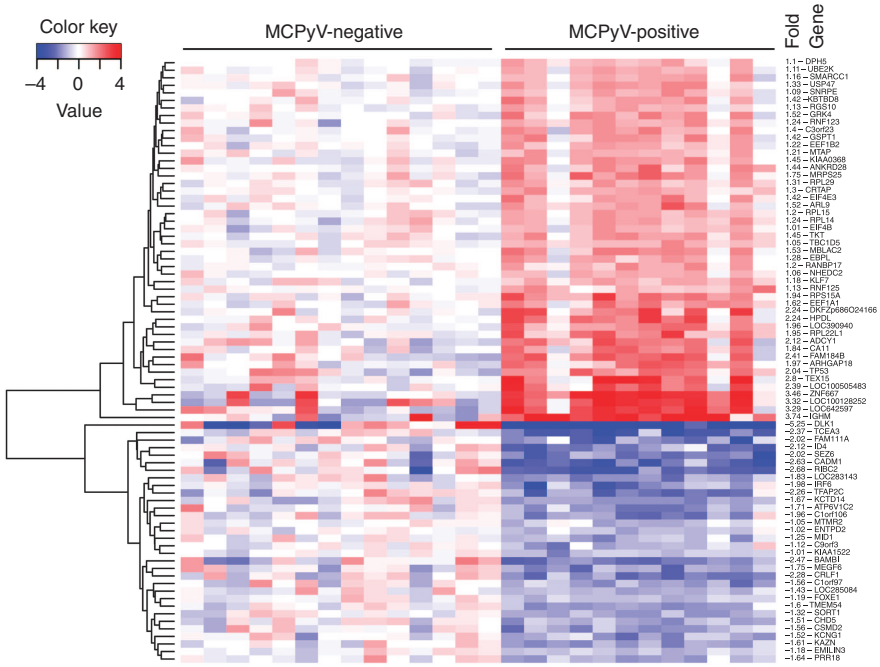

Figure 3. Genes with greatest differential expression in Merkel cell polyomavirus (MCPyV)-positive tumors relative to MCPyV-negative tumors. All genes shown have adjusted *P*-value $\leqslant 0.05$. Fold values are in log2.

Table 2. Functional gene classes enriched in MCPyV-negative compared with MCPyV-positive tumors

KEGG pathway[1], probe set	Gene	Description	Fold[2]
Axon guidance			
229288_at	*EPHA7*	*EPH receptor A7*	4.41
214607_at	*PAK3*	*p21 protein (Cdc42/Rac)-activated kinase 3*	4.72
231325_at	*UNC5D*	*unc-5 homolog D (C. elegans)*	4.29
200965_s_at	*ABLIM1*	*Actin binding LIM protein 1*	3.53
227449_at	*EPHA4*	*EPH receptor A4*	3.27
230425_at	*EPHB1*	*EPH receptor B1*	4.06
209589_s_at	*EPHB2*	*EPH receptor B2*	2.50
236088_at	*NTNG1*	*Netrin G1*	2.36
213169_at	*SEMA5A*	Semaphorin 5A	2.03
223610_at	*SEMA5B*	*Semaphorin 5B*	2.16
32541_at	*PPP3CC*	*Protein phosphatase 3, catalytic subunit, γ isozyme*	0.49
212298_at	*NRP1*	*Neuropilin 1*	0.48
240425_x_at	*ROBO2*	*Roundabout, axon guidance receptor, homolog 2 (Drosophila)*	0.43
227955_s_at	*EFNA5*	*Ephrin-A5*	0.29
213603_s_at	*RAC2*	*rho family, small GTP binding protein Rac2*	0.36
206941_x_at	*SEMA3E*	*Semaphorin 3E*	0.11
Pathways in cancer			
208606_s_at	*WNT4*	*Wingless-type MMTV integration site family, member 4*	3.94
203638_s_at	*FGFR2*	*Fibroblast growth factor receptor 2*	2.75
210512_s_at	*VEGFA*	*Vascular endothelial growth factor A*	2.73
205463_s_at	*PDGFA*	*Platelet-derived growth factor α polypeptide*	2.25
230288_at	*FGF14*	*Fibroblast growth factor 14*	2.06
227271_at	*FGF11*	*Fibroblast growth factor 11*	2.07
227314_at	*ITGA2*	*Integrin, α2 (CD49B, α2 subunit of VLA-2 receptor)*	2.25
221029_s_at	*WNT5B*	*Wingless-type MMTV integration site family, member 5B*	2.04
239178_a	*FGF9*	*Fibroblast growth factor 9 (glia-activating factor)*	0.43
203132_at	*RB1*	*Retinoblastoma 1*	0.41
223709_s_at	*WNT10A*	*Wingless-type MMTV integration site family, member 10A*	0.28
Notch signaling pathway			
224215_s_at	*DLL1*	*Delta-like 1 (Drosophila)*	4.99
201218_at	*CTBP2*	*C-terminal binding protein 2*	2.71
203394_s_at	*HES1*	*Hairy and enhancer of split 1, (Drosophila)*	2.50
32137_at	*JAG2*	*Jagged 2*	2.35
216268_s_at	*JAG1*	*Jagged 1*	2.25
Neuroactive ligand–receptor interaction			
209990_s_at	*GABBR2*	*γ-Aminobutyric acid (GABA) B receptor, 2*	7.94
231192_at	*LPAR3*	*Lysophosphatidic acid receptor 3*	5.98
221107_at	*CHRNA9*	*Cholinergic receptor, nicotinic, α9*	4.41
231384_at	*GRIN2A*	*Glutamate receptor, ionotropic, N-methyl D-aspartate 2A*	2.69
209793_at	*GRIA1*	*Glutamate receptor, ionotropic, AMPA 1*	2.62
213506_at	*F2RL1*	*Coagulation factor II (thrombin) receptor-like 1*	2.30
229944_at	*OPRK1*	*Opioid receptor, κ1*	2.14
229309_at	*ADRB1*	*Adrenergic, β1-, receptor*	2.0
230593_at	*GRIK3*	*Glutamate receptor, ionotropic, kainate 3*	2.03

Table 2 Continued on following page

Table 2. (Continued)

KEGG pathway[1], probe set	Gene	Description	Fold[2]
206128_at	*ADRA2C*	*Adrenergic, α-2C-, receptor*	0.41
205279_s_at	*GLRB*	*Glycine receptor, β*	0.38
211772_x_at	*CHRNA3*	*Cholinergic receptor, nicotinic, α3*	0.36
229686_at	*P2RY8*	*Purinergic receptor P2Y, G-protein coupled, 8*	0.39
213845_at	*GRIK2*	*Glutamate receptor, ionotropic, kainate 2*	0.38
207307_at	*HTR2C*	*5-Hydroxytryptamine (serotonin) receptor 2C*	0.38

Abbreviations: KEGG, Kyoto Encyclopedia of Genes and Genomes; MCPyV, Merkel cell polyomavirus.
[1]KEGG pathways for each gene group are shown in bold. Note that although a functional class/pathway may be upregulated as a whole by KEGG analysis, some individual genes within a class may not display upregulation.
[2]Fold change represents relative array transcript expression in MCPyV-negative Merkel cell carcinoma (MCC) relative to MCPyV-positive MCC. A central value for each probe set was determined by averaging log-transformed data and taking the anti-logarithm.

MCPyV-positive tumors, which did not reach statistical significance (fold 2.4, $P = 0.06$).

RB expression is decreased in MCPyV-negative MCCs

Previous reports have described increased RB protein expression in MCPyV-positive tumors (Bhatia *et al.*, 2010b; Sihto *et al.*, 2011), although other reports found no association (Houben *et al.*, 2010; Schrama *et al.*, 2011). We observed a 2.4-fold upregulation of *RB1* in MCPyV-positive tumors by microarray analysis (Table 2). By immunohistochemistry analysis, 7/7 (100%) MCPyV-positive tumors were diffusely positive (>50% of cells) for the expression of RB protein (Figure 4). In contrast, only 1/14 (7%) MCPyV-negative tumors showed diffuse RB expression, 5 (36%) cases displayed intermediate levels of expression (10–50% of cells), and 8 (57%) lacked significant expression.

DISCUSSION

Transcriptome profiling by DNA microarray analysis is a powerful tool for identifying gene expression changes within tumors and tumor subgroups. Here, we report gene expression profiles of 30 MCCs, with direct comparison to 4 primary cutaneous SCCs and 2 BCCs, as well as *in silico* comparison to 64 normal skin samples. In support of the biological validity of our expression profiles, our screen identified upregulation of diagnostic markers for MCCs, including CK20 and neuroendocrine markers, with respect to normal skin and SCCs. We also identified increased expression of genes that may have protumorigenic roles in MCCs, including *FYN* and *FEV*. Further expression and functional studies are needed to characterize the roles of these genes in MCCs.

Uncertainty regarding the cell of origin for MCCs contributes to the difficulty in understanding the mechanisms of MCC tumorigenesis. Historically, MCC was thought to arise from Merkel cells, which are mechanoreceptor cells in the basal epidermis that share immunohistochemical and ultrastructural features with MCCs. However, this theory has been debated because MCC often spares the epidermis, whereas benign Merkel cells are intraepidermal (Plaza and Suster, 2006; Van Keymeulen *et al.*, 2009). MCCs in our cohort displayed differential regulation of genes with proposed roles in mechanosensation and/or known expression in benign Merkel cells (Haeberle *et al.*, 2004; Chalfie, 2009; Coste *et al.*, 2010; Garrison *et al.*, 2011). In addition, functional gene set analysis identified that MCC was enriched for gene clusters expressed in the inner ear, an organ with known developmental similarities to benign Merkel cells. These findings further demonstrate the similarity between MCCs and benign Merkel cells.

The discovery and characterization of MCPyV has provided a mechanism by which benign Merkel cells or progenitor stem cells may undergo malignant transformation (Becker, 2010). The mechanisms of tumorigenesis in MCPyV-negative MCCs are less clear. Evidence suggests that tumors with low/absent viral DNA and/or lack of LTAg expression are associated with loss of RB expression (Bhatia *et al.*, 2010a, b; Sihto *et al.*, 2011), increased c-KIT expression (Waltari *et al.*, 2011), increased p53 expression (Bhatia *et al.*, 2010b; Waltari *et al.*, 2011), and *TP53* mutations in a subset (Sihto *et al.*, 2011). Although previous studies have performed gene expression microarray analysis of benign mouse Merkel cells, MCC cell lines, and MCC tumors (Haeberle *et al.*, 2004; Paulson *et al.*, 2011; Van Gele *et al.*, 2004), these studies did not compare gene expression profiles of MCPyV-positive and MCPyV-negative tumors.

In MCPyV-positive MCCs, viral LTAg has been shown to promote tumor growth by binding and inactivating the tumor-suppressor protein RB (Shuda *et al.*, 2008; Houben *et al.*, 2012). The role of RB in MCPyV-negative MCC pathogenesis has been unclear, with some studies demonstrating decreased RB expression (Bhatia *et al.*, 2010a; Sihto *et al.*, 2011), whereas others finding no difference (Houben *et al.*, 2010). Our study demonstrated a 2.4-fold lower *RB1* expression in MCPyV-negative tumors relative to MCPyV-positive tumors by gene expression microarray. Perhaps more significantly, the majority of MCPyV-negative MCCs displayed the absence of RB protein expression, whereas RB was diffusely expressed in all MCPyV-positive tumors. Thus, loss of RB activity may be integral to MCC pathogenesis, either through its inactivation by LTAg in MCPyV-positive tumors or by loss of RB expression

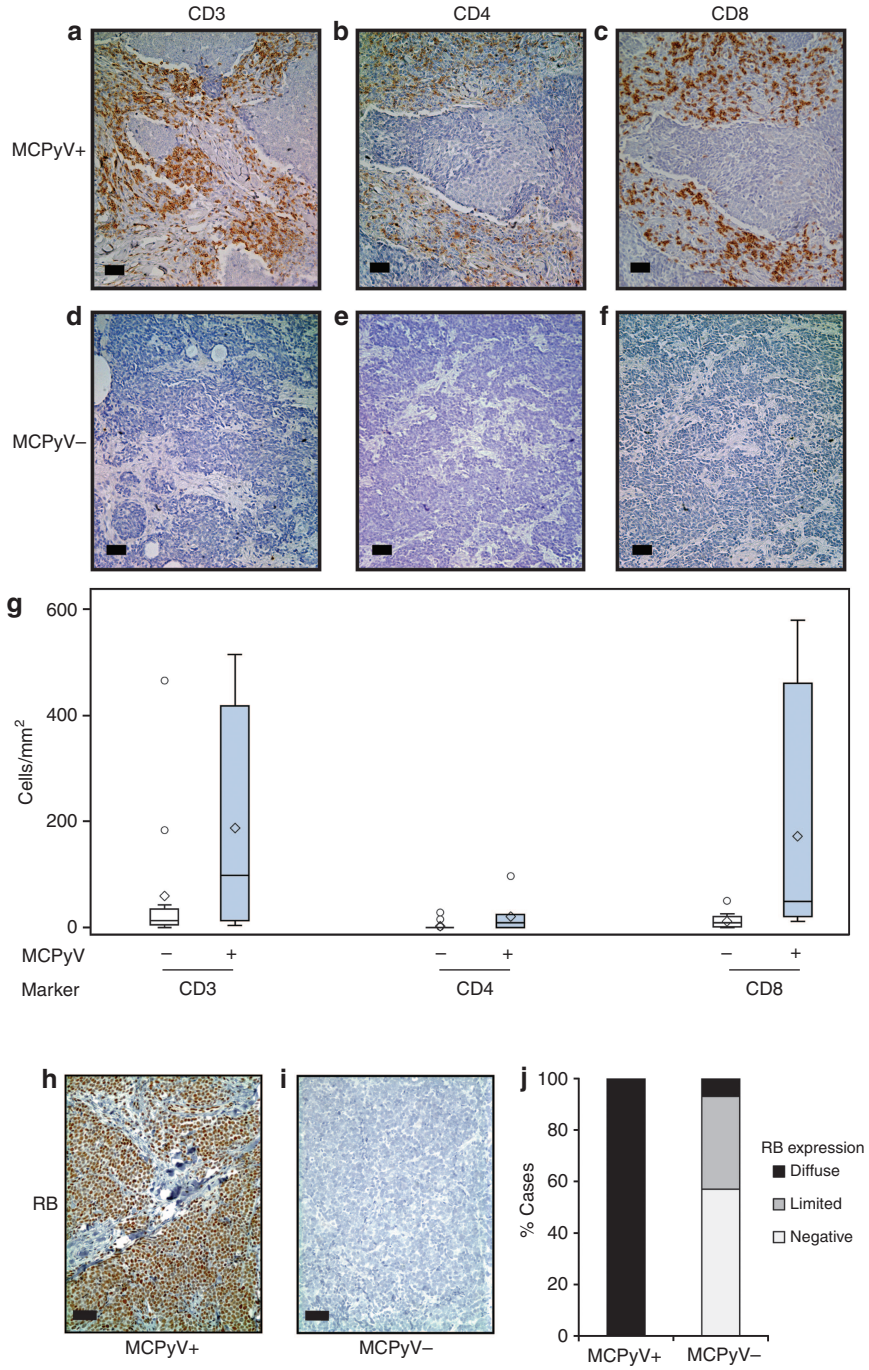

Figure 4. Merkel cell polyomavirus (MCPyV) negativity is associated with relatively decreased immune response and loss of RB expression. Relative to (**a–c**) MCPyV-negative tumors, (**d–f**) MCPyV-positive tumors display a trend toward (**a**, **d**, **g**) increased CD3+ peritumoral lymphocytes, (**b**, **e**, **g**) low CD4+ T lymphocytes, and (**c**, **f**, **g**) significantly increased CD8+ T lymphocytes by immunohistochemistry. (**h**, **j**) MCPyV-positive tumors uniformly express RB, (**i**, **j**) whereas the majority of MCPyV-negative tumors display loss of RB expression by immunohistochemistry. Bar = 50 μm.

in MCPyV-negative tumors. Deletions at the RB locus have been described in MCCs (Leonard and Hayard, 1997; Van Gele *et al.*, 1998; Larramendy *et al.*, 2004; Paulson *et al.*, 2009). A subset of MCPyV-negative tumors retained RB expression, suggesting that an alternative mechanism of RB pathway dysregulation may occur in these tumors.

The relationship of MCPyV status with various clinical parameters is under active investigation. Age and stage at presentation were not significantly related to MCPyV status in our study. In agreement with previous reports (Paik *et al.*, 2011; Sihto *et al.*, 2011), we observed a significantly higher incidence of MCPyV-negative MCC tumors on the head and

neck, whereas more MCPyV-positive MCC tumors were located on the limbs. The incidence of MCPyV by PCR in our cohort was lower (46%) than the commonly reported 70–80% (Bhatia *et al.*, 2011). Because the influence of factors such as immune status and geography on MCPyV incidence in MCC is incompletely understood, we cannot rule out the possibility that clinical/epidemiologic factors are affecting the rate of MCPyV positivity in our cohort.

Several lines of evidence suggest that both cellular and humoral responses occur in response to viral antigens expressed in MCPyV-positive MCCs. Serum antibodies against MCPyV TAg are relatively specific for the presence of active MCCs, whereas antibodies against viral capsid proteins are less specific (Carter *et al.*, 2009; Pastrana *et al.*, 2009; Paulson *et al.*, 2009; Tolstov *et al.*, 2009; Faust *et al.*, 2011). MCPyV-reactive CD4+ and CD8+ T cells have been isolated from MCPyV-positive MCC tumors, but are absent in MCPyV-negative tumors (Iyer *et al.*, 2011). Furthermore, one study found that MCPyV-positive tumors are associated with significantly increased CD3+ and CD8+ TILs, as well as tumor-infiltrating monocytes, although another study did not corroborate these findings with respect to CD8+ T cells (Paulson *et al.*, 2011; Sihto *et al.*, 2012). By GO analysis, we observed increased expression of immune response genes in MCPyV-positive tumors, consistent with the presence of increased tumoral lymphocytes. Immunohistochemistry revealed significantly increased CD8+ T cells in the peritumoral stroma of MCPyV-positive tumors. Together with previous studies, our results indicate that MCPyV-associated cellular immune response appears to consist predominantly of CD8+ lymphocytes (Iyer *et al.*, 2011; Sihto *et al.*, 2012), although we observed the immune response to consist of predominantly peritumoral lymphocytes rather than TILs.

In summary, we report a transcriptome-wide comparison of MCPyV-positive MCCs with MCPyV-negative MCCs. RB expression is lost in the majority of MCPyV-negative tumors, supporting the concept that RB deregulation is a key alteration in MCCs. Our data are in keeping with the notion of two distinct classes of MCCs based on viral status. Further studies evaluating the Notch pathway and receptor tyrosine kinases are underway to elucidate their role in the pathogenesis of MCCs.

MATERIALS AND METHODS

Tumor procurement and cell lines

Studies were approved by the Institutional Review Board of the University of Michigan. For all tumors, MCC diagnosis was confirmed by morphology and immunohistochemistry at the time of diagnosis. All tumor tissues were procured from the University of Michigan Hospitals Cutaneous Surgery and Oncology Program. At the time of collection, tumor tissue was flash-frozen in liquid nitrogen and stored at $-80\,^{\circ}C$ until RNA extraction. Formalin-fixed, paraffin-embedded tissue for tissue microarray construction was obtained from archival tissue blocks. The adequacy of frozen section and paraffin-embedded tissue was confirmed by two pathologists (DRF and PWH).

RNA was prepared from normal skin and processed for microarray analysis as previously described (Gudjonsson *et al.*, 2009).

The MCC cell lines were established at the University of Michigan from tumor tissue procured as described above, with additional details on cell line establishment in Supplementary Materials and Methods online.

RNA isolation

Areas with at least 70% tumor cellularity were targeted for RNA isolation, using hematoxylin and eosin stains obtained on frozen sections for each specimen. Representative 2-mm^3 areas were removed from the tissue block and homogenized in the presence of Trizol reagent (Life Technologies, Gaithersburg, MD), and total cellular RNA was purified according to the manufacturer's standard protocol. RNA was then further purified using miRVANA (Ambion, Austin, TX) according to the manufacturer's protocol. After purification, RNA quality was assessed by Agilent Bioanalyzer (Agilent, Santa Clara, CA).

cRNA synthesis and gene expression profiling

Human 133 Plus 2.0 microarrays (Affymetrix, Santa Clara, CA) were used, which consist of $>54{,}000$ probe sets representing $\sim 47{,}400$ transcripts. Preparation of cRNA hybridization was performed according to the manufacturer's protocols. GeneChips were scanned using the Affymetrix 3000 7G GeneChip Scanner with Autoloader and processed by the Affymetrix Gene Chip Command Console version 3.2. Samples were analyzed in two batches, with overlapping specimens included to control for batch effect. Because of the lack of overlapping samples, batch effect could not be corrected for the *in silico* comparison between MCCs and normal skin. Expression data have been made available in the Gene Expression Omnibus (GEO) database (accession number GSE39612).

Statistical analysis

For DNA microarrays, log2 gene expression values were calculated using a robust multiarray average. Adjusted *P*-value was calculated using the Benjamini and Hochberg False Discovery Rate concept (Benjamini and Hochberg, 1995). For all analyses, a fold change of $\geqslant 2.0$ or $\leqslant 0.5$ with an adjusted *P*-value of $\leqslant 0.05$ was considered statistically significant. Array quality was evaluated by standard error estimates for each gene standardized across all arrays after fitting a probe level model using the affyPLM package of Bioconductor (Bolstad *et al.*, 2005). One sample was eliminated owing to elevated standard errors. Age was described and tested between MCPyV-positive and MCPyV-negative groups using means, SD, and corresponding *t*-tests. Anatomical site was compared between MCPyV groups with Fisher's exact test. Further details on statistical analyses are provided in Supplementary Materials and Methods online.

Characterization of MCPyV status in MCC tumors

PCR of isolated genomic tumor DNA was performed to detect the presence of MCPyV DNA in tumor samples. Because tumors that contain MCPyV DNA but lack LTAg expression are reported to be more similar to MCPyV-negative tumors with regard to clinical outcome (Sihto *et al.*, 2011), we also characterized RNA expression of MCPyV LTAg and STAg by reverse transcription PCR. Tumor RNA was used to prepare complementary DNA according to standard protocols. Briefly, 0.25 μg of RNA was used for first-strand complementary DNA synthesis with SuperScript II Reverse Transcriptase (Invitrogen, Carlsbad, CA) as per the manufacturer's

instructions. Detection of MCPyV sequence (based on GenBank NC_010277) was conducted by semiquantitative PCR on tumor complementary DNA and/or genomic DNA using primers TA1, targeting the exon 1 coding region common to all T antigen transcripts (forward primer: nucleotides (nts) 226–245, reverse primer: nts 357–376), and TA2, targeting the exon 1 coding region specific to STAg only (forward primer: nts 354–373, reverse primer: nts 571–590). Results were further confirmed using the previously described primers for capsid viral protein (VP1) (Feng *et al.*, 2008). Human β-actin primers were used as a control. As a control for a gene expressed in MCC, primers were used for atonal homolog 1 (GenBank NP_005163; forward primer: nts 230–249, reverse primer: nts 444–463). All primers were designed using Primer3 (http://fokker.wi.mit.edu/primer3/input.htm). PCR products were separated by agarose gel and visualized by ethidium bromide. Three tumors were excluded owing to insufficient tissue or degraded DNA. An additional tumor was excluded because of equivocal results for TAg mRNA expression. Of the remaining 26 tumors, 12 (46%) had both MCPyV DNA and mRNA, and 14 (54%) lacked both MCPyV DNA and mRNA.

Immunohistochemistry

A tissue microarray of profiled tumors was constructed, with each tumor represented by two 1.0-mm cores. Tumor content of each core was verified by hematoxylin and eosin staining. Immunohistochemistry was performed using a DAKO automated stainer (DAKO, Carpinteria, CA) as previously described (Yu *et al.*, 2010). Antibodies and dilutions are described in Supplementary Materials and Methods online.

For RB, the percentage of tumor cells labeled was recorded as one of three categories: $<10\%$ (negative), 10–50% (intermediate), and $>50\%$ (diffuse). All positive cases displayed a nuclear pattern of staining. RB staining was compared between MCPyV groups with Fisher's exact test.

For CD20, CD3, CD4, and CD8, peritumoral lymphocytes and TILs were counted across two 1-mm tissue microarray cores for each tumor. Wilcoxon rank test was used to test differences in CD20+, CD3+, CD4+, and CD8+ peritumoral lymphocyte and TIL measures between MCPyV groups.

CONFLICT OF INTEREST

The authors state no conflict of interest.

ACKNOWLEDGMENTS

This work was supported by the Anatomic Pathology Project Fund of the University of Michigan Department of Pathology, a Research Career Development Award from the Dermatology Foundation (to MEV), a Training Grant in Cell and Molecular Dermatology (T32AR007197; to KTN), and NIH grant R01CA087837 (to AAD).

SUPPLEMENTARY MATERIAL

Supplementary material is linked to the online version of the paper at http://www.nature.com/jid

REFERENCES

Ames HM, Bichakjian CK, Liu GY *et al.* (2011) Huntingtin-interacting protein 1: a Merkel cell carcinoma marker that interacts with c-Kit. *J Invest Dermatol* 131:2113–20

Becker JC (2010) Merkel cell carcinoma. *Ann Oncol* 21(Suppl 7):vii81–5

Becker JC, Houben R, Ugurel S *et al.* (2009) MC polyomavirus is frequently present in Merkel cell carcinoma of European patients. *J Invest Dermatol* 129:248–50

Ben-Arie N, Hassan BA, Bermingham NA *et al.* (2000) Functional conservation of atonal and Math1 in the CNS and PNS. *Development* 127:1039–48

Benjamini Y, Hochberg Y (1995) Controlling the false discovery rate: a practical and powerful approach to multiple testing. *J R Stat Soc Ser B Stat Methodol* 57:289–300

Bhatia K, Goedert JJ, Modali R *et al.* (2010a) Immunological detection of viral large T antigen identifies a subset of Merkel cell carcinoma tumors with higher viral abundance and better clinical outcome. *Int J Cancer* 127:1493–6

Bhatia K, Goedert JJ, Modali R *et al.* (2010b) Merkel cell carcinoma subgroups by Merkel cell polyomavirus DNA relative abundance and oncogene expression. *Int J Cancer* 126:2240–6

Bhatia S, Afanasiev O, Nghiem P (2011) Immunobiology of Merkel cell carcinoma: implications for immunotherapy of a polyomavirus-associated cancer. *Curr Oncol Rep* 13:488–97

Bichakjian CK, Lowe L, Lao CD *et al.* (2007) Merkel cell carcinoma: critical review with guidelines for multidisciplinary management. *Cancer* 110:1–12

Bolstad B, Collin F, Brettschneider J *et al.* (2005) Quality assessment of Affymetrix GeneChip data. In: Gentleman R, Carey V, Huber W, Irizarry R, Dudoit S eds *Bioinformatics and Computational Biology Solutions Using R and Bioconductor*. Springer: New York, 183–326

Brewer JD, Shanafelt TD, Otley CC *et al.* (2012) Chronic lymphocytic leukemia is associated with decreased survival of patients with malignant melanoma and Merkel cell carcinoma in a SEER population-based study. *J Clin Oncol* 30:843–9

Brunner M, Thurnher D, Pammer J *et al.* (2008) Expression of VEGF-A/C, VEGF-R2, PDGF-alpha/beta, c-kit, EGFR, Her-2/Neu, Mcl-1 and Bmi-1 in Merkel cell carcinoma. *Mod Pathol* 21:876–84

Carter JJ, Paulson KG, Wipf GC *et al.* (2009) Association of Merkel cell polyomavirus-specific antibodies with Merkel cell carcinoma. *J Natl Cancer Inst* 101:1510–22

Chalfie M (2009) Neurosensory mechanotransduction. *Nat Rev Mol Cell Biol* 10:44–52

Coste B, Mathur J, Schmidt M *et al.* (2010) Piezo1 and Piezo2 are essential components of distinct mechanically activated cation channels. *Science* 330:55–60

Cui C, Elsam T, Tian Q *et al.* (2004) Gli proteins up-regulate the expression of basonuclin in Basal cell carcinoma. *Cancer Res* 64:5651–8

Engels EA, Frisch M, Goedert JJ *et al.* (2002) Merkel cell carcinoma and HIV infection. *Lancet* 359:497–8

Faust H, Pastrana DV, Buck CB *et al.* (2011) Antibodies to Merkel cell polyomavirus correlate to presence of viral DNA in the skin. *J Infect Dis* 203:1096–100

Feng H, Shuda M, Chang Y *et al.* (2008) Clonal integration of a polyomavirus in human Merkel cell carcinoma. *Science* 319:1096–100

Fernandez-Figueras MT, Puig L, Musulen E *et al.* (2007) Expression profiles associated with aggressive behavior in Merkel cell carcinoma. *Mod Pathol* 20:90–101

Foulongne V, Kluger N, Dereure O *et al.* (2008) Merkel cell polyomavirus and Merkel cell carcinoma, France. *Emerg Infect Dis* 14:1491–3

Garneski KM, Warcola AH, Feng Q *et al.* (2009) Merkel cell polyomavirus is more frequently present in North American than Australian Merkel cell carcinoma tumors. *J Invest Dermatol* 129:246–8

Garrison SR, Dietrich A, Stucky CL (2011) TRPC1 contributes to light-touch sensation and mechanical responses in low-threshold cutaneous sensory neurons. *J Neurophysiol* 107:913–22

Gudjonsson JE, Ding J, Li X *et al.* (2009) Global gene expression analysis reveals evidence for decreased lipid biosynthesis and increased innate immunity in uninvolved psoriatic skin. *J Invest Dermatol* 129:2795–804

Haeberle H, Fujiwara M, Chuang J *et al.* (2004) Molecular profiling reveals synaptic release machinery in Merkel cells. *Proc Natl Acad Sci USA* 101:14503–8

He H, Fang W, Liu X *et al.* (2009) Frequent expression of glypican-3 in Merkel cell carcinoma: an immunohistochemical study of 55 cases. *Appl Immunohistochem Mol Morphol* 17:40–6

Hers I, Vincent EE, Tavare JM (2011) Akt signalling in health and disease. *Cell Signal* 23:1515–27

Houben R, Adam C, Baeurle A *et al.* (2012) An intact retinoblastoma protein-binding site in Merkel cell polyomavirus large T antigen is required for promoting growth of Merkel cell carcinoma cells. *Int J Cancer* 130:847–56

Houben R, Schrama D, Alb M *et al.* (2010) Comparable expression and phosphorylation of the retinoblastoma protein in Merkel cell polyoma virus-positive and negative Merkel cell carcinoma. *Int J Cancer* 126:796–8

Iyer JG, Afanasiev OK, McClurkan C *et al.* (2011) Merkel cell polyomavirus-specific CD8+ and CD4+ T-cell responses identified in merkel cell carcinomas and blood. *Clin Cancer Res* 17:6671–80

Kasper M, Jaks V, Hohl D *et al.* (2012) Basal cell carcinoma - molecular biology and potential new therapies. *J Clin Invest* 122:455–63

Kassem A, Schopflin A, Diaz C *et al.* (2008) Frequent detection of Merkel cell polyomavirus in human Merkel cell carcinomas and identification of a unique deletion in the VP1 gene. *Cancer Res* 68:5009–13

Katano H, Ito H, Suzuki Y *et al.* (2009) Detection of Merkel cell polyomavirus in Merkel cell carcinoma and Kaposi's sarcoma. *J Med Virol* 81:1951–8

Kennedy MM, Blessing K, King G *et al.* (1996) Expression of bcl-2 and p53 in Merkel cell carcinoma. An immunohistochemical study. *Am J Dermatopathol* 18:273–7

Kuhajda FP, Olson JL, Mann RB (1986) Merkel cell (small cell) carcinoma of the skin: immunohistochemical and ultrastructural demonstration of distinctive perinuclear cytokeratin aggregates and a possible association with B cell neoplasms. *Histochem J* 18:239–44

Laga AC, Lai CY, Zhan Q *et al.* (2010) Expression of the embryonic stem cell transcription factor SOX2 in human skin: relevance to melanocyte and merkel cell biology. *Am J Pathol* 176:903–13

Larramendy ML, Koljonen V, Bohling T *et al.* (2004) Recurrent DNA copy number changes revealed by comparative genomic hybridization in primary Merkel cell carcinomas. *Mod Pathol* 17:561–7

Leonard JH, Cook AL, Van Gele M *et al.* (2002) Proneural and proneuroendocrine transcription factor expression in cutaneous mechanoreceptor (Merkel) cells and Merkel cell carcinoma. *Int J Cancer* 101:103–10

Leonard JH, Hayard N (1997) Loss of heterozygosity of chromosome 13 in Merkel cell carcinoma. *Genes Chromosomes Cancer* 20:93–7

Moll I, Gillardon F, Waltering S *et al.* (1996) Differences of bcl-2 protein expression between Merkel cells and Merkel cell carcinomas. *J Cutan Pathol* 23:109–17

Nakayama T, Higuchi T, Oiso N *et al.* (2012) Expression and function of FRA2/JUND in cutaneous T-cell lymphomas. *Anticancer Res* 32:1367–73

Paik JY, Hall G, Clarkson A *et al.* (2011) Immunohistochemistry for Merkel cell polyomavirus is highly specific but not sensitive for the diagnosis of Merkel cell carcinoma in the Australian population. *Hum Pathol* 42:1385–90

Pastrana DV, Tolstov YL, Becker JC *et al.* (2009) Quantitation of human seroresponsiveness to Merkel cell polyomavirus. *PLoS Pathog* 5:e1000578

Paulson KG, Iyer JG, Tegeder AR *et al.* (2011) Transcriptome-wide studies of merkel cell carcinoma and validation of intratumoral CD8+ lymphocyte invasion as an independent predictor of survival. *J Clin Oncol* 29:1539–46

Paulson KG, Lemos BD, Feng B *et al.* (2009) Array-CGH reveals recurrent genomic changes in Merkel cell carcinoma including amplification of L-Myc. *J Invest Dermatol* 129:1547–55

Penn I, First MR (1999) Merkel's cell carcinoma in organ recipients: report of 41 cases. *Transplantation* 68:1717–21

Peter M, Couturier J, Pacquement H *et al.* (1997) A new member of the ETS family fused to EWS in Ewing tumors. *Oncogene* 14:1159–64

Plaza JA, Suster S (2006) The Toker tumor: spectrum of morphologic features in primary neuroendocrine carcinomas of the skin (Merkel cell carcinoma). *Ann Diagn Pathol* 10:376–85

Plettenberg A, Pammer J, Tschachler E (1996) Merkel cells and Merkel cell carcinoma express the BCL-2 proto-oncogene. *Exp Dermatol* 5:183–8

Ramsay RG, Gonda TJ (2008) MYB function in normal and cancer cells. *Nat Rev Cancer* 8:523–34

Saito YD, Jensen AR, Salgia R *et al.* (2010) Fyn: a novel molecular target in cancer. *Cancer* 116:1629–37

Schrama D, Peitsch WK, Zapatka M *et al.* (2011) Merkel cell polyomavirus status is not associated with clinical course of Merkel cell carcinoma. *J Invest Dermatol* 131:1631–8

Shuda M, Feng H, Kwun HJ *et al.* (2008) T antigen mutations are a human tumor-specific signature for Merkel cell polyomavirus. *Proc Natl Acad Sci USA* 105:16272–7

Shuda M, Kwun HJ, Feng H *et al.* (2011) Human Merkel cell polyomavirus small T antigen is an oncoprotein targeting the 4E-BP1 translation regulator. *J Clin Invest* 121:3623–34

Sihto H, Bohling T, Kavola H *et al.* (2012) Tumor infiltrating immune cells and outcome of Merkel cell carcinoma: a population-based study. *Clin Cancer Res* 18:2872–81

Sihto H, Kukko H, Koljonen V *et al.* (2011) Merkel cell polyomavirus infection, large T antigen, retinoblastoma protein and outcome in Merkel cell carcinoma. *Clin Cancer Res* 17:4806–13

Su LD, Fullen DR, Lowe L *et al.* (2002) CD117 (KIT receptor) expression in Merkel cell carcinoma. *Am J Dermatopathol* 24:289–93

Tan PY, Chang CW, Chng KR *et al.* (2012) Integration of regulatory networks by NKX3-1 promotes androgen-dependent prostate cancer survival. *Mol Cell Biol* 32:399–414

Tolstov YL, Pastrana DV, Feng H *et al.* (2009) Human Merkel cell polyomavirus infection II. MCV is a common human infection that can be detected by conformational capsid epitope immunoassays. *Int J Cancer* 125:1250–6

Van Gele M, Boyle GM, Cook AL *et al.* (2004) Gene-expression profiling reveals distinct expression patterns for Classic versus Variant Merkel cell phenotypes and new classifier genes to distinguish Merkel cell from small-cell lung carcinoma. *Oncogene* 23:2732–42

Van Gele M, Speleman F, Vandesompele J *et al.* (1998) Characteristic pattern of chromosomal gains and losses in Merkel cell carcinoma detected by comparative genomic hybridization. *Cancer Res* 58:1503–8

Van Keymeulen A, Mascre G, Youseff KK *et al.* (2009) Epidermal progenitors give rise to Merkel cells during embryonic development and adult homeostasis. *J Cell Biol* 187:91–100

Waltari M, Sihto H, Kukko H *et al.* (2011) Association of Merkel cell polyomavirus infection with tumor p53, KIT, stem cell factor, PDGFR-alpha and survival in Merkel cell carcinoma. *Int J Cancer* 129:619–28

Yu L, Harms PW, Pouryazdanparast P *et al.* (2010) Expression of the embryonic morphogen Nodal in cutaneous melanocytic lesions. *Mod Pathol* 23:1209–14